2010 American Control Conference
Marriott Waterfront, Baltimore, MD, USA
June 30-July 02, 2010

Application of frequential properties of power systems to robustness analysis

Alvaro Giusto

***Abstract*— This paper studies the application of certain frequency domain properties of a class of power systems to the robustness analysis. The small signal models of a significant class of power systems-namely, systems without resistive losses nor excitation control–was recently shown to meet passivity-like, convex conditions in the frequency domain. A classical benchmark is considered and it is shown that the presence of excitation control and resistive elements does not completely destroy the above-mentioned property, which remains valid in the frequency band associated to the electromechanical modes. The example includes a detailed robustness analysis showing the importance of the *a priori* knowledge of the frequential properties of these models in the frequency band of interest.**

I. Introduction

The complexity of power system dynamics has stimulated the seek for analysis tools that take advantage of structural dynamic properties of these systems [1], [3], [18], [19]. These antecedents provide us with a set of techniques–also named direct methods–based in the energy function that have been used in the stability analysis of power systems. Its applications ranges from estimation of stability domains and critical clearing times to online techniques for the detection of loss of synchronism [2], [16].

More recently, some progresses have been reported by applying a more fundamental concept: the theory of dissipative dynamical systems [11],[20]. Basically, a dissipative system satisfies a balance between the storage of a generalized internal energy and a suitably defined supply rate function that describes the interchanges with the environment. These fundamental ideas are strongly related with concepts like passivity and finite gain, and constitute a fundamental basis of the development of the robustness analysis, see [15] and references therein. References [7], [17] report applications of the dissipativity ideas to power systems. The approach taken in this paper is strongly related with previous works [6], [7], [8], [9] where the specific concept of dissipativity made way for the analysis of frequential properties of small signal models of a class of power systems. This class is defined by the interconnection of several shunt devices comprising:

- generic ZIP model for reactive power loads,
- constant active power loads,
- classical, second order, synchronous machine model,
- third order, synchronous machine model,[9],
- several FACT devices, [2],
- detailed, sixth order, model of synchronous machine with constant excitation [8],

through lossless transmission lines As a consequence of the above-mentioned results, these systems satisfy a special case of Integral Quadratic Constraint (IQC) that provides us a very versatile framework for the robustness analysis [15].

We consider a classical benchmark for stability studies of power systems, comprising a two area, four machine system, see [14]. Simplifying assumptions are taken for the area 2, ensuring the complete fulfillment of the mentioned IQC while a conventional model is supposed for the area 1, which includes conventional synchronous generators and a Static Var Compensator, SVC. The voltage regulator of this device is designed in order to meet standard tracking requirements and the preservation of the IQC at a frequency band. Significant parametric variations are assumed in the model, whose robustnesss is investigated through the search of suitable IQC multipliers. It is shown that the *a priori* knowledge of the original IQC multiplier is a valuable tool for the assessment of robust stability in the presence of electromechanical modes and its associated resonance.

The paper is organized as follows. Section II presents the basic framework for the power system modeling. Section III introduces the frequential properties of the small signal models of the above-mentioned class of power systems. Section IV presents the example, that includes controller design and closed loop stability analysis. We wrap up the paper with some concluding remarks.

II. Power System Modeling

Each bus has an associated identifier $j \in J_B := \{1, .., m\}$. The interconnection with external systems is modeled by the power injections at a set of buses $J_E \subset J_B$. We will make reference to a set $J_\alpha \subset J_B$ in order to define a subsystem. The respective cardinalities of the sets J_E, J_α are $m_E, m_\alpha \leq m$.

The stability analysis of power systems is typically done with the help of RMS[1] models that are described through a set of algebraic differential equations of the type

$$\left\{ \begin{array}{lcl} \dot{x} &=& f(x,y) \\ 0 &=& g(x,y) \end{array} \right. \qquad (1)$$

with $x \in \mathbb{R}^n$ the state vector and $y \in \mathbb{R}^{2m}$ the set of link variables given by the voltage phasor en each bus:

$$y_j := \left[\begin{array}{c} \theta_j \\ V_j \end{array} \right]; j \in J_B. \qquad (2)$$

Alvaro Giusto is with the IIE, Facultad de Ingeniería, Universidad de la República, Montevideo, Uruguay. alvaro@fing.edu.uy

[1]We refer to the fundamental frequency, balanced, models usually employed in the study of power systems stability, see [14].

978-1-4244-7425-7/10/$26.00 ©2010 AACC

We are interested in the study of the stability of the interconnection between adjacent electrical subsystems. So, we need to model the external power injections to a given subsystem or area. Be the vector

$$\mathrm{u}_e^E = \begin{bmatrix} P_e^E \\ Q_e^E \end{bmatrix} \in \mathbb{R}^2, e \in J_E \tag{3}$$

with P_e^E, Q_e^E the active and reactive power injected into the system at the bus $e \in J_E$ by external systems. This interaction can be done at a set of several buses. However, in this paper we consider a single frontier bus to keep simple the notation . Thus, we consider $J_E = \{e\}$ and the external power injection to the subsystem is denoted

$$u^E := u_e^E.$$

Accordingly, the voltage phasor at the frontier bus is $y^E := y_e$. In this way, a subsystem can be modeled by a description as the following:

$$\begin{cases} \dot{x}_\alpha &= f_\alpha(x_\alpha, y_\alpha, u^E) \\ 0 &= g_\alpha(x_\alpha, y_\alpha, u^E) \end{cases} \tag{4}$$

with $x_\alpha \in \mathbb{R}^{n_\alpha}$ the state vector of the devices connected to the buses in J_α and $y_\alpha \in \mathbb{R}^{2m_\alpha}$ the corresponding link variables. We define the set $\mathcal{D} \in \mathbb{R}^{n_\alpha} \times \mathbb{R}^{2m_\alpha} \times \mathbb{R}^2$ where the solutions of the DAE are unique and well defined [10]:

$$\mathcal{D} \triangleq \{(x, y, u) | g(x, y, u) = 0 \; and$$

$$\nabla_y g(x, y, u) is \; nonsingular\}.$$

From a input/output point of view, the subsystem can be seen alternatively as an operator $u^E \to y^E$ or an operator $y^E \to u^E$, provided that the triad $(x, y, u) \in \mathcal{D}$.

Several recent references, see [6], [7], [8], have studied the dynamic properties of a class of subsystems that can be described in a Hamiltonian-like form as

$$\begin{cases} \dot{x}_\alpha &= (J - R)\nabla_x S_\alpha(x_\alpha, y_\alpha) \\ 0 &= \nabla_{y_\alpha} S_\alpha(x_\alpha, y_\alpha) + B_u(y_e)u^E \end{cases} \tag{5}$$

with $S_\alpha : \mathbb{R}^{n_\alpha} \times \mathbb{R}^{2m_\alpha}$ the storage function. $J = -J^\top \in \mathbb{R}^{n_\alpha \times n_\alpha}$ and $R = R^\top \geq 0, R \in \mathbb{R}^{n_\alpha \times n_\alpha}$ are constant matrices and $B_u : \mathbb{R}^2 \to \mathbb{R}^{2\times 2}$

$$B_u(y_i) \triangleq \begin{bmatrix} 1 & 0 \\ 0 & \frac{1}{V_i} \end{bmatrix}. \tag{6}$$

The function S_α coincides with the classical energy function, see e.g. [18], when simplified models are considered for the synchronous machines. The use of the term *storage function* is related with the dissipativity properties studied for this class of systems and it is justified in references [6], [9].

As it was mentioned in the Introduction, the class of power systems that satisfies (5) consists, between others, of several shunt devices :

A1. generic ZIP model for reactive power loads,
A2. constant active power loads,
A3. classical, second order, synchronous machine model,
A4. several FACT devices,

interconnected through lossless Π models of transmission lines and transformers.

III. INPUT-OUTPUT PROPERTIES FOR SMALL SIGNAL MODELS

Variables at the equilibrium will be denoted with a supra-index $\star$: $x^\star, y^\star, u^\star$, etc. The incremental variables around the equilibrium point will be denoted with a tilde: $\tilde{x} = x - x^\star, \tilde{y} = y - y^\star, \tilde{u} = u - u^\star$, etc. Denote $\mathcal{W} := B_u(y_e^\star)$, i.e.

$$\mathcal{W} = \begin{bmatrix} 1 & 0 \\ 0 & \frac{1}{V_e^\star} \end{bmatrix}.$$

The linear map $\tilde{u}^E \to \tilde{y}^E$ of subsystem (4) or (5) will be represented by the matrix transfer function[2] $\Sigma : \mathcal{C} \to \mathcal{C}^{2\times 2}$:

$$\hat{y}^E(s) = \Sigma(s)\hat{u}^E(s). \tag{7}$$

Analogously, the inverse map $\Gamma(s) = \Sigma(s)^{-1}$ describes

$$\hat{u}^E(s) = \Gamma(s)\hat{y}^E(s). \tag{8}$$

Under mild conditions, the dissipativity of systems satisfying (5) imply a frequency-dependent inequality that is stated in next proposition. See [9] for a complete demonstration.

Proposition 1: Assume that the small signal model $\Sigma(s)$ of (5) around the equilibrium satisfies $\Sigma(j\omega) \in R\mathcal{L}_\infty$. Then

$$\begin{bmatrix} I \\ \Sigma(j\omega) \end{bmatrix}^* \Pi_d(j\omega) \begin{bmatrix} I \\ \Sigma(j\omega) \end{bmatrix} \geq 0 \;\; \forall w \in \mathbb{R} \tag{9}$$

$$\Pi_d(j\omega) := |h(j\omega)|^2 \begin{bmatrix} 0 & -j\omega\mathcal{W}^\top \\ j\omega\mathcal{W} & 0 \end{bmatrix} \tag{10}$$

for all function $h(s)$ real rational stable and strictly proper.

Remark 1: Equations (9), (10) describe a convex frequency-weighted passivity-like condition for Σ.

Define, to facilitate the notation, the quadratic forms $\sigma_l : \mathcal{C}^{2\times 2} \times \mathcal{C}^{4\times 4} \to \mathcal{C}^{2\times 2}$:

$$\sigma_l(H, \Pi) := \begin{bmatrix} I_2 \\ H \end{bmatrix}^* \Pi \begin{bmatrix} I_2 \\ H \end{bmatrix},$$

and $\sigma_u : \mathcal{C}^{2\times 2} \times \mathcal{C}^{4\times 4} \to \mathcal{C}^{2\times 2}$:

$$\sigma_u(G, \Pi) := \begin{bmatrix} G \\ I_2 \end{bmatrix}^* \Pi \begin{bmatrix} G \\ I_2 \end{bmatrix}.$$

Remark 2: It is convenient to mention that the adoption of $\tilde{y}^E, \tilde{u}^E$ as, respectively, the output and the input is merely conventional. The inequality (9) can be written

$$\sigma_l(\Sigma(j\omega), \Pi_d(j\omega)) \geq 0 \; \forall \omega \in \mathbb{R}.$$

If we pre and post multiply this inequality by Γ^* and Γ being $\Gamma(j\omega) = \Sigma(j\omega)^{-1}$, and use the block structure of multiplier Π_d we get a set of conditions equivalent to (9):

$$\sigma_u(\Gamma(j\omega), \Pi_d(j\omega)) \geq 0 \; \forall \omega \in \mathbb{R} \Leftrightarrow$$

$$\sigma_l(\Gamma(j\omega), \Pi_d(j\omega)) \leq 0 \; \forall \omega \in \mathbb{R} \Leftrightarrow$$

$$\sigma_u(-\Gamma(j\omega), \Pi_d(j\omega)) \leq 0 \; \forall \omega \in \mathbb{R}. \tag{11}$$

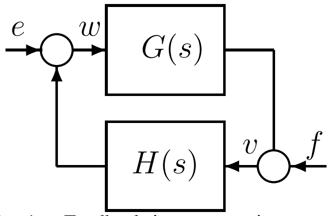

Fig. 1. Feedback interconnection

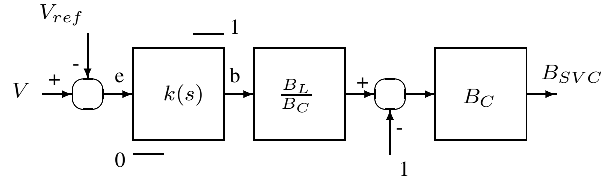

Fig. 2. Basic model of the SVC

A. Stability analysis of linear feedback interconnections

Denote $G \star H$ the operator $(e, f) \to (v, w)$ defined by the standard feedback interconnection

$$\left\{ \begin{array}{lcl} v & = & Gw + f \\ w & = & Hv + e \end{array} \right. . \tag{12}$$

G and H are two linear, time-invariant operators with transfer functions $G(s), H(s) \in \mathbf{R}\mathcal{L}_\infty^{2\times 2}$ and stabilizable and detectable state space realizations. The interconnection is assumed well-possed. The following proposition is a particular formulation of the IQC theorem, [15], specialized for our special case[3]

Proposition 2: Let $G(s), H(s) \in \mathbf{R}\mathcal{H}_\infty^{2\times 2}$ such that the operator $G \star H$ is also stable. Assume the existence of a multiplier $\Pi(j\omega) \in \mathbf{R}\mathcal{L}_\infty^{4\times 4}$ such that

i. $\sigma_l(H(j\omega), \Pi(j\omega)) \geq 0 \; \forall\omega$

ii. there exists $\epsilon > 0$ such that

$$\sigma_u(G(j\omega), \Pi(j\omega)) \leq -\epsilon I, \; \forall\omega \in \mathbb{R}, \tag{13}$$

$$iii. \qquad \begin{bmatrix} 0 \\ I \end{bmatrix}^* \Pi(j\omega) \begin{bmatrix} 0 \\ I \end{bmatrix} \leq 0, \; \forall\omega \in \mathbb{R}. \tag{14}$$

Then, the feedback interconnection $G \star \mathcal{H}$ is stable for all linear, time invariant, stable operator satisfying

$$\sigma_l(\mathcal{H}(j\omega), \Pi(j\omega)) \geq 0 \; \forall\omega \tag{15}$$

The proof is straightforward by writing $G \star \mathcal{H}$ as the interconnection of a nominal stable system $G \star H$ with the block $\Delta := \mathcal{H} - H$ and applying the IQC theorem.

Remark 3: Denote $\mathcal{S}_\Pi$ the set of operators $\mathcal{H} \in \mathbf{R}\mathcal{H}_\infty^{2\times 2}$ satisfying (15). It is easy to see that condition (14) implies the convexity of $\mathcal{S}_\Pi$.

The value of Proposition 2–a simple reformulation of the IQC theorem–resides in that the nominal stability can be extended to a convex set defined by the involved multiplier.

IV. Example

Consider the system depicted in Fig. **??**, Example 12.6 in [14] which is split in two areas, with the bus 8 at the frontier. Linear models for both areas were computed with DSAT [12], by taking y_8 and u_8 as the interconnection variables.

[2]We denote $\hat{z}(s)$ the Laplace transform of the small signal variable $\tilde{z}(t)$.

[3]The assumptions on the linear maps and their respective realizations imply the equivalence between the input-output and inner stability, see [4].

The model of area 1 has the same parameters as [14], included the non-zero machine resistances and transfer conductances. The excitation systems of machines G1 and G2 are given in [14] and provide a high transient gain plus a standard setting for the *power system stabilizer*, PSS.

The SVC comprises a fixed capacitor (200 MVAr) and a 0-200 MVAr thyristor-controlled reactor (TCR), whose voltage regulator will be designed to ensure a proper voltage tracking and to improve the stability robustness.

The area 2 is modeled fully in accordance with Assumptions A1-A4: the resistive losses in transmission lines are neglected, classical second order models are considered for generators G_3 and G_4. On the other hand, significant parametric variations are considered for this area.

The signal $\tilde{u}_8$, see Fig. **??**, is taken as input to area 2. As a result of this convention and definitions (7) and (8) for each area, the system depicted in Fig. **??** can be described as the feedback interconnection of $H = \Sigma_2$ and $G = -\Gamma_1$.

A. Design of the SVC voltage regulator

The SVC is modeled as in Fig. 2 where the controller $k(s)$ includes a fixed time constant due to the converter. The controller $k(s)$ must ensure the closed loop stability and the tracking requirements given by the slope of the voltage characteristic (set to 7 %) and a prescribed phase margin of approx. 45 degrees. See the chapter 11 in [14] for a precise technical presentation of these requirements.

Due to Proposition 1, area 2 satisfies

$$\sigma_l(\Sigma_2(j\omega), \Pi_d(j\omega)) \geq 0 \; \forall\omega.$$

Our objective is the design of the regulator $k(s)$ to ensure

$$\sigma_u(-\Gamma_1(j\omega), \Pi_d(j\omega)) \leq -\epsilon I, \forall\omega \in \Omega \tag{16}$$

for a set $\Omega \in \mathbb{R}$ as broad as possible. Notice that, in absence of control and resistive losses, condition (16) would be true for $\epsilon = 0$ for all $\omega \in \mathbb{R}$, due to (11). The presence of excitation control, resistive loads and transmission losses restrict the band of frequencies where condition (16) is valid or feasible through the controller design.

The constraints that (16) imposes on the gain $k(j\omega)$ for several frequencies are depicted in Fig. 3. The constraints were shown to be feasible for $\Omega = [\omega_l, \omega_h] = [0.38, \; 9.94]$. This set can not be extended for lower frequencies due to voltage slope constraints nor for higher frequencies due to bandwidth limitations associated to the phase margin. However, this set Ω is, significantly, wide enough to include the system electromechanical local and interarea modes which

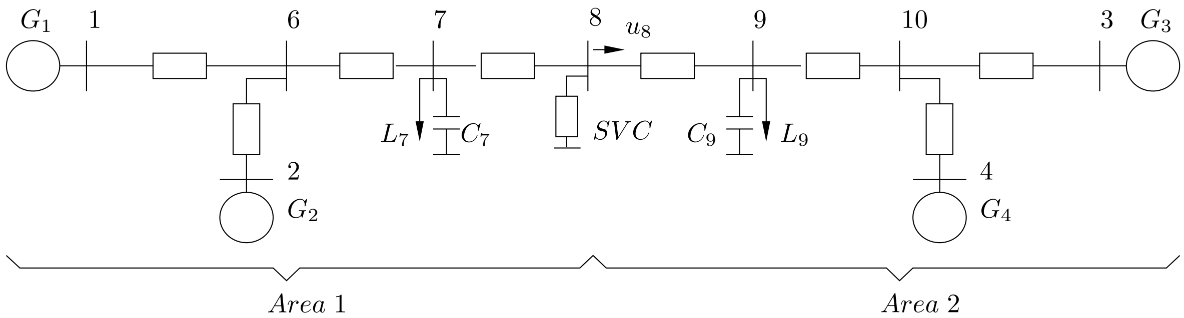

range from 0.5 to 1.1 Hz (3.1 to 6.9 rad/sec). The resulting SVC voltage regulator is given by

$$k(s) = \frac{6.5(s+1)}{(0.1s+1)(0.02s+1)}.$$

The plots in Figs. 4 show the resulting eigenvalues of the matrix $\sigma_u(-\Gamma_1(j\omega), \Pi_d(j\omega))$.

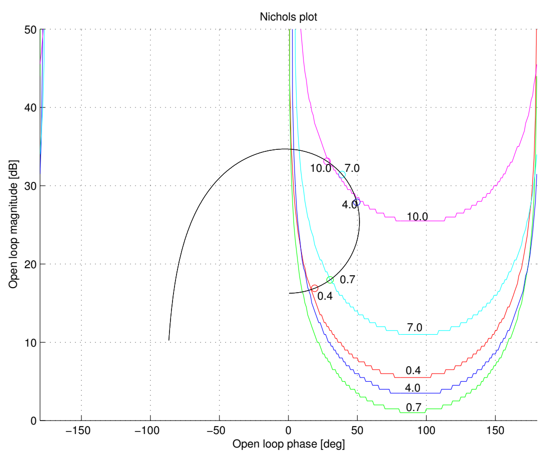

Fig. 3. *SVC Voltage regulator design. Nichols plot of* $k(j\omega)$ *and feasibility regions for* $\omega = \{0.1, 0.4, 0.7, 4.0, 7.0\}$ *rad/sec.*

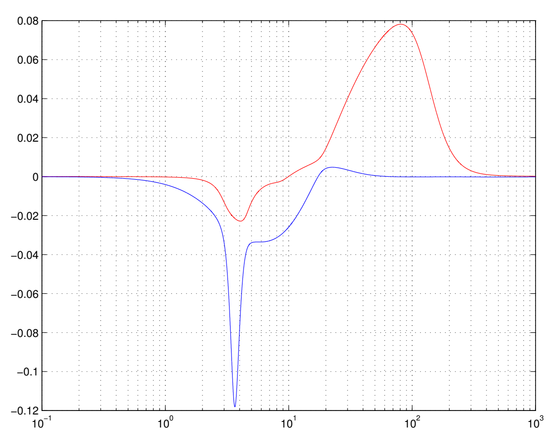

Fig. 4. *Frequency domain condition for area 1. Eigenvalues of* $\sigma_u(-\Gamma_1(j\omega), \Pi_d(j\omega))$.

B. *Modeling of parametric uncertainty in area 2*

A set of scenarios for area 2 were considered, which are associated to two parameters: the voltage dependence of load L_9 and the transient reactance of machine G3. The reactive load $L9$ is supposed either constant impedance (case A), constant current (case B) or constant reactive power (case C). The transient reactance of G_3 is supposed to be $X'_d \in [0.3, \lambda]$, with $\lambda \geq 0.3$ a figure of merit useful to compare some alternative approaches for the robustness analysis.

The choice of a set of eight values for the parameter X'_d and three for load L_9 results in $N = 24$ scenarios, each defined by the matrices (A_i, B_i, C_i, D_i) of the standard state space linear model. The corresponding matrices

$$M_i := \begin{bmatrix} A_i & B_i \\ C_i & D_i \end{bmatrix}, \ i = 1..N.$$

were approximated by the set

$$M_i = M_1 + \begin{bmatrix} P_1 \\ P_2 \end{bmatrix} \Delta_i [Q_1 \ Q_2]; i = 1..N$$

with $\Delta_i \in R^{p \times p}, i = 1..N$, with the help of an elementary singular value decomposition. The minimum size p for a good approximation is closely related with the number of independent parameters. In our case $p = 2$ was sufficient.

Finally, the area 2 is modeled as

$$\begin{bmatrix} \dot{x} \\ y_8 \end{bmatrix} = \left[M_1 + \begin{bmatrix} P_1 \\ P_2 \end{bmatrix} \Delta [Q_1 \ Q_2] \right] \begin{bmatrix} x \\ u_8 \end{bmatrix},$$

with the uncertain bock Δ given by the polytope associated to the N scenarios already described:

$$\Delta = \sum_{r=1}^{r=N} \alpha_r \Delta_r, \sum_r \alpha_r = 1, \alpha_r \geq 0. \qquad (17)$$

This model constitutes a linear fractional transformation (LFT) of the nominal block $N(s)$ and the uncertain block Δ depicted in Fig. 5, with

$$N(s) = \left[\begin{array}{c|cc} A_1 & P_1 & B_1 \\ \hline Q_1 & 0 & Q_2 \\ C_1 & P_2 & D_1 \end{array} \right].$$

So, the uncertain system can be seen either as the interconnection of Δ and[4] $F_l(N, -\Gamma_1)$ at interface B, or

[4]Reference [21] provides a complete framework for LFTs and its manipulation. $F_l(N, -\Gamma_1)$ denotes the lower linear fractional transformation between block N and $-\Gamma_1$, see Fig. 5.

the interconnection of $F_u(N, \Delta)$ with $-\Gamma_1$ at the interface A. Notice that the model (17) considers all the possible combinations of the continuous variations of parameter X'_d and the ZIP model for load L_9.

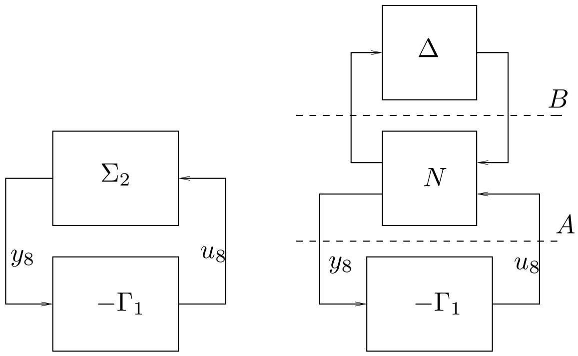

Fig. 5. Feedback interconnections between subsystems Γ_1 and Σ_2.

C. Robustness analysis

The stability of the interconnection of area 1 and 2—the last given by equation (17)—is analyzed with the help of Proposition 2. Notice that both areas and the block N are stable. The problem is the computation of a suitable multiplier Π satisfying condition i) to iii). The multiplier Π_d satisfies conditions i) and iii). However, it does not solve the problem since condition ii) is only satisfied for $\omega \in \Omega$.

Given the polytope description (17) for the area 2, it is convenient to consider the standard family of multipliers $\Pi_{pol} \in \mathbb{R}^{4\times4}$, see [15]:

$$\Pi_{pol} = \begin{bmatrix} Q & F \\ F^\top & R \end{bmatrix}; Q = Q^\top; R = R^\top \tag{18}$$

such that

$$R \leq 0; \;\; Q + F\Delta_r + \Delta_r^\top F^\top + \Delta_r^\top R\Delta_r > 0, \forall r = 1..N. \tag{19}$$

In a first instance, the search for a suitable multiplier satisfying Proposition 2 was carried with multipliers of the family Π_{pol}. More, precisely, the following computational problem was solved:

Problem 1 Find $\Pi_{pol}^{\mathbb{R}}$ and $\epsilon > 0$ satisfying (18), (19) and

$$\sigma_u(F_l(N, -\Gamma_1)(j\omega), \Pi_{pol}^{\mathbb{R}}) \leq -\epsilon I, \forall \omega \in \mathbb{R}.$$

Problem 1 was formulated as a LMI via the KYP lemma, see [15], and solved with the software [5]. The extreme λ for which the robust stability could be established is shown in Table I. For comparison purposes, the stability was also studied by the computation of the eigenvalues of the dynamic matrix at a fine grid of scenarios. The extreme value, denote λ_{MAX} is also listed in Table I. As it can be observed, the analysis of robust stability based only with multiplier $\Pi_{pol}^{\mathbb{R}}$ is quite conservative. It is worth to notice that the analysis based in the multipliers Π_{pol} would be able to guarantee the stability for time variant blocks Δ, see [15], which is a broader set of uncertainty than the original N scenarios. The family Π_{pol} is taken as a benchmark and its use is justified by the relative simplicity of the computation involved.

In a second instance the search was confined to the frequency weighted sum of two members $\Pi_{pol}^{lf}, \Pi_{pol}^{hf}$ of the family Π_{pol}, trying to exploit[5] the fact that the multiplier Π_d satisfies condition i), ii) and iii) of Proposition 1 in a band Ω. So, the structure of the multiplier Π was chosen

$$\Pi_{d+pol} = \mathbf{w}_{lf}(\omega)\Pi_{pol}^{lf} + \mathbf{w}_{hf}(\omega)\Pi_{pol}^{hf}$$

being the weights $\mathbf{w}_{lf}, \mathbf{w}_{hf}$ given by

$$\mathbf{w}_{lf} = \begin{cases} 1 & if \; |\omega| < \omega_l \\ 0 & otherwise \end{cases}; \; \mathbf{w}_{hf} = \begin{cases} 1 & if \; |\omega| > \omega_h \\ 0 & otherwise \end{cases}.$$

In this way, the computation of the multiplier can now be relaxed to the following problem:

Problem 2 Find the multipliers $\Pi_{pol}^{lf}, \Pi_{pol}^{hf}$ and $\epsilon > 0$ satisfying (18), (19) and

$$\sigma_u(F_l(N, -\Gamma_1)(j\omega), \Pi_{pol}^{lf}) \leq -\epsilon I, \forall |\omega| < \omega_l,$$

$$\sigma_u(F_l(N, -\Gamma_1)(j\omega), \Pi_{pol}^{hf}) \leq -\epsilon I, \forall |\omega| > \omega_h.$$

Problem 2 is a frequency dependent LMI valid *in a restricted domain* and therefore other theoretical tools–different from the classical KYP lemma–are needed. Reference [13] provides an effective framework for this type of problems that enables us to formulate the Problem 2 as a LMI. The maximum λ for which Problem 2 is feasible was computed and is listed in Table I.

As it can be seen, the procedure of splitting the frequency domain in three regions and taking into account the multiplier Π_d improved noticeably the results of the analysis. However, it is convenient to know if the improvement is due to the splitting in regions or to the use of multiplier Π_d. So, it was also computed the maximum λ such that the following problem remains feasible:

Problem 3 Find Π_{pol}^{Ω} and $\epsilon > 0$ satisfying (18), (19) and

$$\sigma_u(F_l(N, -\Gamma_1)(j\omega), \Pi_{pol}^{\Omega}) \leq -\epsilon I, \forall \omega \in \Omega.$$

The result can be read in Table I and seems to indicate that the difficulties in the assessment of robust stability with multipliers Π_{pol} resides precisely in the band Ω associated to the electromechanical modes and the associated resonances. The exploitation of multiplier Π_d, derived by analytical methods and valid in a sensible frequency band, allows to significantly improve the results of the analysis.

TABLE I

EXTREME VALUES OF λ FOR EACH TECHNIQUE OF ANALYSIS

Problem 1 ($\Pi_{pol}^{\mathbb{R}}$)	Problem 2 (Π_{d+pol})	Problem 3 (Π_{pol}^{Ω})	Stability λ_{MAX}
0.32	2.53	0.32	2.548

Figure 6 displays the stability regions associated to each choice of multiplier. Significantly, the gap between the hard

[5]The stability can be easily proved through the use of multiplier Π_d in band Ω at interface A and multiplier Π_{d+pol} in $\bar{\Omega}$ at interface B.

stability limit and the region able to be predicted by the simultaneous use of multiplier Π_{pol} and Π_d is very small.

Figure 7 depicts the loci of the most significant modes of the interconnection when x'_d varies in the interval $[0.3, 2.8]$ and the load L_9 is modeled with constant reactive power. The local mode of area 1 remains unchanged as expected, and the local mode of area 2 and inter-area mode vary significantly but without crossing the imaginary axis because Proposition 1 is valid for a suitable frequency band Ω. The stability is lost when a real mode turns unstable for values of $\lambda \geq \lambda_{MAX}$.

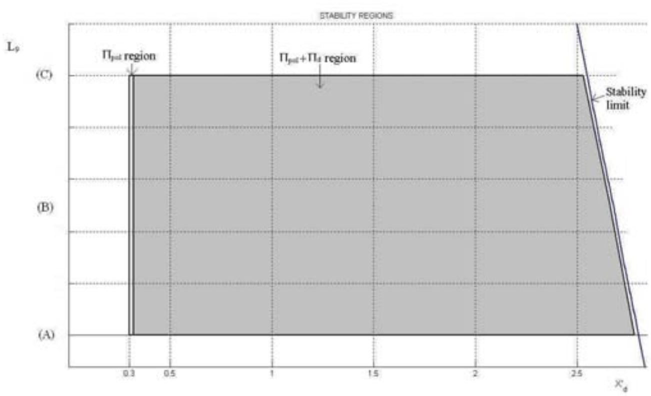

Fig. 6. Stability regions.

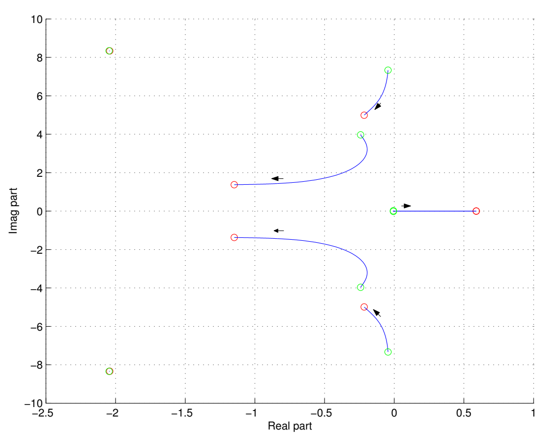

Fig. 7. *Eigenvalue loci for power flow C,* $X'_d \in [0.3, 2.8]$.

V. Concluding remarks

The effects of the dissipativity properties of power systems on the frequency response of these systems was explored with the help of a classical example. A first conclusion is that these properties remain valid, for realistic models, in a very significant band of frequencies, associated to the electromechanical modes. It was also shown that SVC devices can contribute positively to these properties, without any adverse effect on its standard tracking requirements. Finally, a careful robustness analysis was carried on the example. The results support the idea that the *a priori* knowledge of the system behavior in the frequency band associated to the electromechanical modes greatly simplifies the robustness analysis and improves the results of this type of analysis.

References

[1] T. Athay, R. Podmore, and S. Virmani. A practical method for the direct analysis of transient stability. *IEEE Trans. on Power App. Syst.*, pages 573–582, Mar 1979.

[2] V. Azbe, U. Gabrijel, D. Povh, and R Mihalic. The energy function of a general multimachine system with a unified power flow controller. *IEEE Transactions on Power Systems*, 20(3):1478–1485, 2005.

[3] A. Bergen and D. Hill. A structure preserving model for power system stability analysis. *IEEE Trans Power App. Syst.*, PAS 100(1):25–35, 1981.

[4] C-T. Chen. *Linear system theory and design*. Holt, Rinehart and Winston, Inc, 1984.

[5] P. Gahinet; A. Nemirovski; A. Laub; M. Chilali. *LMI Control Toolbox For Use with MATLAB*, 1995.

[6] A. Giusto. On some dissipativity properties of a class of power system models. *3rd. IFAC Symposium on System, structure and Control, Foz de Iguazú*, 2007.

[7] A. Giusto, R. Ortega, and A. Stankovic. On transient stabilization of power system: a power–shaping solution for structure–preserving models. In *IEEE Conf. on Decision and Control*, San Diego, USA, Dec. 2006.

[8] A. Giusto, A. Stankovic, and R. Ortega. Dissipativity properties of detailed models of synchronous generators. In *IEEE Conference on Decision and Control*, Cancún, México, December 2008.

[9] Alvaro Giusto. On some frequency domain properties of small signal models of a class of power systems. In *IEEE Conference on Decision and Control, 46th. Florida, USA*, dec 2007.

[10] D. Hill and I. Mareels. Stability theory for differential/algebraic systems with application to power systems. *IEEE Trans. Circ. and Syst.*, 37(11):1416–1423, 1990.

[11] D. J. Hill and P. J. Moylan. Dissipative dynamical systems: Basic input–output and state properties. *Journal of the Franklin Institute*, 309(5):327–357, 1980.

[12] Powertech Labs Inc. Dsatools. dynamic security assessment software. *www.powertechlabs.com*.

[13] T. Iwasaki and S. Hara. Generalized kyp lemma: Unified frequency domain inequalities with design applications. *IEEE Transactions on Automatic Control*, 50:41–59, 2005.

[14] P. Kundur. *Power Systems Stability and Control*. McGraw-Hill, New York, 1994.

[15] A. Megretski and A. Rantzer. System analysis via integral quadratic constraints. *IEEE TAC*, 42(6):819–830, June 1997.

[16] K.R. Padiyar and S. Krishna. Online detection of loss of synchronism usin energy function criterion. *IEEE Trans. on Power Delivery*, 21(1):46–55, Jan 2006.

[17] A.M. Stankovic, P.C. Stefanov, G. Tadmor, and D.J. Sobajic. Dissipativity as a unifying control design framework for suppression of low frequency oscillations in power systems. *IEEE Transactions on Power Systems*, 14(1):192–199, Feb. 1999.

[18] N.A. Tsolas, A. Arapostathis, and P.P. Varaiya. A structure preserving energy function for power system transient stability analysis. *IEEE Transactions on Circuits and Systems*, 32:1041–1049, 1985.

[19] P. Varaiya, F.F. Wu, and Chen R.-L. Direct methods for transient stability analysis of power systems: Recent results. *Proceedings of the IEEE*, 73(12):1703–1715, December 1985.

[20] J.C. Willems. Dissipative dynamical systems. part i: General theory; part II: Linear systems with quadratic supply rates. *Arch. Rational Mech. Anal.*, 45:321–393, 1972.

[21] K. Zhou, J.C. Doyle, and K. Glover. *Robust and Optimal Control*. Prentice-Hall, 1996.